ACS OMEGA

http://pubs.acs.org/journal/acsodf

Article

Gemdimethyl Peptide Nucleic Acids (*α*/*β*/*γ*-*gdm*-PNA): E/Z-Rotamers Influence the Selectivity in the Formation of Parallel/Antiparallel *gdm*-PNA:DNA/RNA Duplexes

Pradnya Kulkarni, Dhrubajyoti Datta, and Krishna N. Ganesh*

Cite This: *ACS Omega* 2022, 7, 40558−40568

Read Online

ACCESS | Metrics & More | Article Recommendations | Supporting Information

ABSTRACT: Peptide nucleic acids (PNAs) consist of an aminoethylglycine (*aeg*) backbone to which the nucleobases are linked through a tertiary amide group and bind to complementary DNA/RNA in a sequence-specific manner. The flexible *aeg* backbone has been the target for several chemical modifications of the PNA to improve its properties such as specificity, solubility, etc. PNA monomers exhibit a mixture of two rotamers (Z/E) arising from the restricted rotation around the tertiary amide N−CO bond. We have recently demonstrated that achiral gemdimethyl substitution at the *α*, *β*, and *γ* sites on the *aeg* backbone induces exclusive Z (*α*-*gdm*)- or E-rotamer (*β*-*gdm*) selectivity at the monomer level. It is now shown that *γ*/*β*-*gdm*-PNA:DNA parallel duplexes are more stable than the analogous antiparallel duplexes, while *γ*/*β*-*gdm*-PNA:RNA antiparallel duplexes are more stable than parallel duplexes. Furthermore, the *γ*/*β*-*gdm*-PNA:RNA duplexes are more stable than the *γ*/*β*-*gdm*-PNA:DNA duplexes. These results with *γ*/*β*-*gdm*-PNA are the reverse of those previously seen with *α*-*gdm*-PNA oligomers that stabilized *antiparallel* *α*-*gdm*-PNA:DNA duplexes compared to *α*-*gdm*-PNA:RNA duplexes. The stability of antiparallel/parallel PNA:DNA/RNA duplexes is correlated with the preference for Z/E-rotamer selectivity in *α*/*β*-*gdm*-PNA monomers, with Z-rotamers (*α*-*gdm*) leading to antiparallel duplexes and E-rotamers (*β*/*γ*-*gdm*) leading to parallel duplexes. The results highlight the role and importance of Z- and E-rotamers in controlling the structural preferences of PNA:DNA/RNA duplexes.

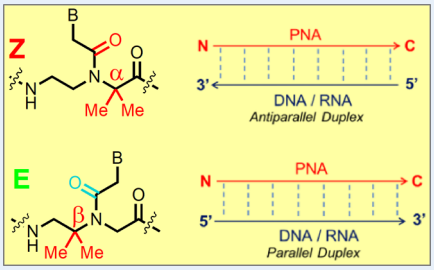

INTRODUCTION

Peptide nucleic acids (PNA) are achiral mimics of nucleic acids composed of a polyamide backbone with recurring units of 2-aminoethylglycine (*aeg*) to which nucleobases A, C, T, and G are linked via a tertiary amide linkage[1,2] (Figure 1). Such a backbone with linear and flexible C−C and C−N bonds has the capacity to reorganize slowly into the preferred conformation for hybridization with both complementary DNA or RNA with similar avidity and a high sequence specificity.[3−6] These characteristics of PNAs combined with their chemical stability to proteases and nucleases and low toxicity provide resourceful applications for in vitro diagnostics and antisense therapeutics.[7−14] The poor cell penetration of PNAs has prompted a number of chemical modifications to effectively improve their properties for hybridization specificity and biological applications.[15−25] PNAs and their analogues have also been finding numerous applications in materials science.[26−29] While the structural role of the linear *aeg* backbone in modulating hybridization properties of PNAs is well documented, the role of the *t*-amide group that has restricted rotation around the N−CO bond linking the base with the *aeg* backbone has not been well studied.

Preorganizing the *aeg*-PNA backbone into a "hybridization-competent conformation" imparts entropic gain in tuning its structure for selective or preferential binding to DNA/RNA.[16] Furthermore, PNA can bind to DNA in either parallel or antiparallel orientations defined by the relative orientations of PNA/DNA strands (Figure 1).[3−6] Several efforts from this laboratory[16−21] and that of others[6,23−30] on structural modifications of the aminoethylglycine (*aeg*) PNA backbone have led to a host of acyclic, cyclic, and chiral backbone-modified assortment of PNA analogues. An interesting rational modification of the *aeg*-PNA backbone is the introduction of *cis*-1,2-disubstituted cyclopentyl[17] and cyclohexyl[18] moieties to match the dihedral angle of the lone C*β*-C*γ* bond in the ethylenediamine segment to 60° as found in the X-ray structure of the PNA:RNA duplex.[31] This results in remarkable discrimination in binding of PNA with isosequential complementary DNA and RNA with preference for binding to RNA. Imparting chirality into the *aeg*-PNA backbone has also shown selectivity for binding DNA in either parallel or antiparallel modes depending on the nature of modifications.[16,19] These approaches demonstrate that the presence of steric constrains and chirality may induce tuning of the PNA backbone to populate hybridization-competent conformations

Received: September 9, 2022
Revised: October 5, 2022
Accepted: October 17, 2022
Published: October 28, 2022

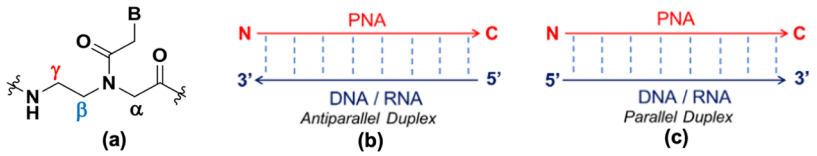

Figure 1. Structure of aminoethylglycl (*aeg*) PNA and relative orientations of parallel and antiparallel PNA:DNA/RNA duplexes (a) and *aeg*-PNA (b) antiparallel and (c) parallel PNA:DNA/RNA duplexes.

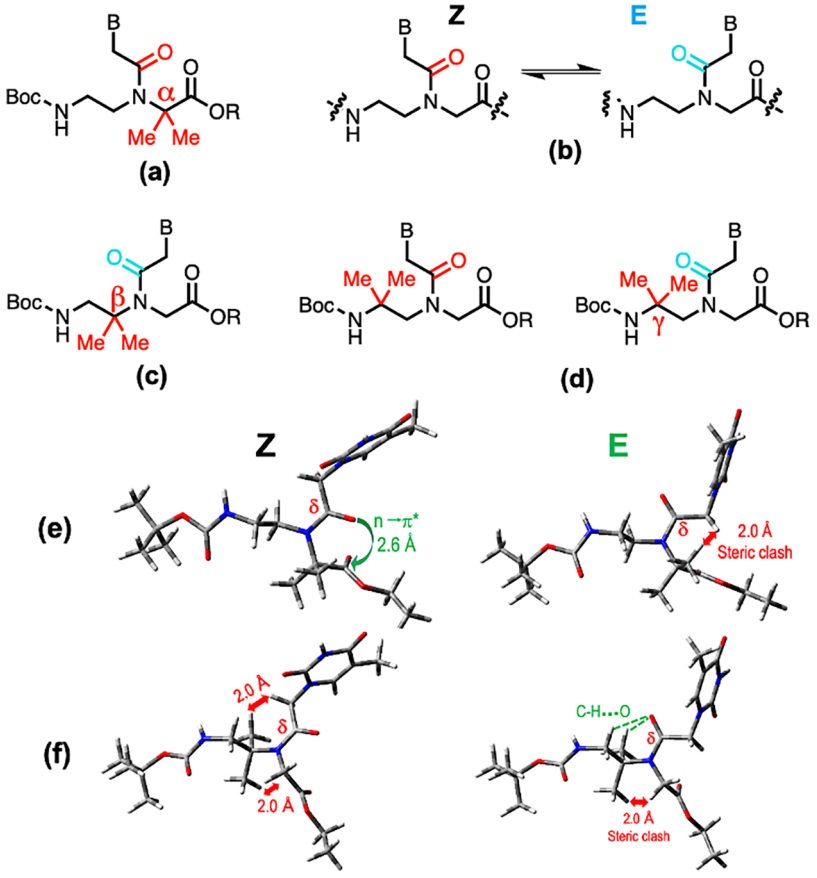

Figure 2. Structures of *α*-, *β*-, and *γ*-*gdm* PNA monomers and their computed Z/E-rotamer structures (a) *α*-*gdm*, (b) Z and E-rotamer equilibrium in *aeg*-PNA, (c) *β*-*gdm*, and (d) *γ*-*gdm* PNA. B = thymine (T) and *t*-amide carbonyl: red (Z-rotamer) and green (E-rotamer). Computed structures of (e) Z/E-*α*-*gdm*-PNA and (f) Z/E-*β*-*gdm*-PNA. Nonbonded interactions marked in red (destabilizing) and green (stabilizing).

for prompting selectivity in binding with DNA/RNA. The introduction of cationic and hydrophilic side chains has led to improved solubility and enhanced cell uptake.[20,21,26−28,32]

A simpler way to impart steric constrains without introducing chirality is to incorporate *gem*-dimethyl substitution into the flexible *aeg* backbone of PNA. A number of *α*-isoaminobutyric acid (*aib*)-containing polypeptides occur naturally, and the *gem*-dimethyl substitution on *α*-carbon of glycine is well-known to promote helicity in peptides.[33] This feature provides us a rationale for the design, synthesis, and study of *α*-gemdimethyl(*gdm*)-PNA (Figure 2a) having *gdm* in the glycine segment of aminoethylglycine PNA.[34] The *α*-*gdm*-PNA-T_n homo-oligomer exhibits significant stabilization of the derived triplex (*α*-*gdm*PNA-T_n)$_2$:dA_n, and duplex *α*-*gdm*-PNA:DNA/RNA from the mixed-base sequence shows a higher T_m relative to that of analogous isosequential RNA duplexes.[34] These results motivated us to explore the specific properties of *gdm* substitution at the *β*- and *γ*-sites on the *aeg* backbone in PNA-T monomers.

Unsubstituted *aeg*-PNA monomers exhibited a mixture of two rotamers (major Z:minor E, 60:40) arising from the restricted rotation around the N−CO *t*-amide bond, with the Z-rotamer corresponding to *δ*-carbonyl pointing to glycine (C-terminus) and E-rotamer having *δ*-carbonyl toward the ethylenediamine (N-terminus) side (Figure 2b).[35−38] In *gdm*-PNA T monomers, it was surprisingly found that the *α*-*gdm* substitution exhibited exclusively the Z-rotamer (Figure 2a), while the *β*-gdm substitution showed exclusively the E-rotamer (Figure 2c).[39] The *γ*-*gdm* substitution (Figure 2d) gave a mixture of minor Z- and major E-rotamers, reverse of that seen in unsubstituted *aeg*-PNA monomers.[39] The relative stabilities of Z- and E-rotamers (Figures 2e and f) were dictated by balance of repulsive steric clashes (red) and nonbonding attractive n → *π** or C−H···O interactions (green).[39] Thus, the Z-rotamer (Figure 2e/Z) was favored for the *α*-*gdm*-PNA monomer and the E-rotamer (Figure 2f/E) is favored for the *β*-*gdm*-PNA monomer.[39] Although at the monomer level, *aeg*-PNA shows a mixture of Z- and E-rotamers, the crystal structure studies at the oligomer level and in duplexes show

https://doi.org/10.1021/acsomega.2c05873
ACS Omega 2022, 7, 40558−40568

that the t-amide bond is always present as Z-rotamer in antiparallel duplexes.[40−43]

PNA analogues with substitutions (both cyclic and acyclic) at Cγ and Cα positions are well known,[15−27] and examples of acyclic PNAs bearing substitution at the Cβ position are rare.[44,45] With the *β-gdm*-PNA T monomer showing exclusively E-rotamers,[39] it would be interesting to study its comparative hybridization and orientation specificity with complementary DNA/RNA at the oligomer level. The work reported in this article demonstrates that the nature of the Z/E-rotamer determines the orientation bias in binding to DNA/RNA and interestingly plays a role in preferentially stabilizing parallel or antiparallel duplexes. While *α-gdm*-PNA with exclusive Z-rotamer stabilized antiparallel duplexes,[34] it is shown here that *β-gdm*-PNA having the E-rotamer predominantly stabilized parallel duplexes over the antiparallel duplexes, reverse of that found in unsubstituted *aeg*-PNA.

RESULTS AND DISCUSSION

The *β-gdm* (Figure 2c) and *γ-gdm* (Figure 2d) *aeg* PNA monomers synthesized as reported before[34,39] were used for the solid-phase synthesis of PNA oligomers on MBHA (4-methyl benzhydrylamine) resin using a Boc strategy starting from the C-terminus to the N-terminus.[46] The orthogonally protected (Boc/Cbz)-L-lysine was first coupled to the resin at the C-terminus, and the synthesis was continued using protected monomers (**c**) or (**d**) for coupling. The in situ activation of the acid function was done with PyBOP. The completion of each coupling reaction was monitored by Kaiser's test[47,48] followed by deprotection of the N-*t*-Boc group using TFA. The Cγ- and Cβ-*gdm*-T monomers (Figure 2c,d) were incorporated at the T-sites in the *aeg*-PNA sequence H-G<u>T</u>AGA<u>T</u>CAC<u>T</u>-NH_2 having three equally spaced thymine residues (Table 1). The same sequence was chosen as that studied earlier incorporating C*α-gdm* substitution[34] to enable the relative comparison of *α-*, *β-*, and *γ-gdm* substituent-dependent effects on duplex formation by the *gdm*-PNA oligomers. To study the sequence-dependent effects of Cβ/Cγ-*gdm* substitutions, PNA oligomers with single modification at the N-terminus (T2), middle (T6), and C-terminus (T10) along with double (T2, T6) and triple (T2, T6, T10) were synthesized (Table 1). After the synthesis, the PNA oligomers were cleaved from the resin by treatment with TFA/TFMSA, which also deprotected the bases, purified by reverse-phase HPLC, and characterized by MALDI-TOF mass spectral data (Supporting Information).

Table 1. PNA Oligomers with Modified/Unmodified Monomers at Various Positions and Orientations in Antiparallel and Parallel PNA:DNA Duplexes[a]

		PNA sequence
entry	sequence code	1 2 3 4 5 6 7 8 9 10
1	*aeg* PNA **1**	H-G T A G A T C A C T-$LysNH_2$
2	*γ gdm*-t^2 PNA **2**	H-G <u>t</u> A G A T C A C T-$LysNH_2$
3	*γ gdm*-t^6 PNA **3**	H-G T A G A <u>t</u> C A C T-$LysNH_2$
4	*γ gdm*-$t^{2,6}$ PNA **4**	H-G <u>t</u> A G A <u>t</u> C A C T-$LysNH_2$
5	*γ gdm*-$t^{2,6,10}$ PNA **5**	H-G <u>t</u> A G A <u>t</u> C A C <u>t</u>-$LysNH_2$
6	*β gdm*-t^2 PNA **6**	H-G <u>t</u> A G A T C A C T-$ysNH_2$
7	*β gdm*-t^6 PNA **7**	H-G T A G A <u>t</u> C A C T-$LysNH_2$
8	*β gdm*-$t^{2,6}$ PNA **8**	H-G <u>t</u> A G A <u>t</u> C A C T-$LysNH_2$
9	*β gdm*-$t^{6,10}$ PNA **9**	H-G T A G A <u>t</u> C A C <u>t</u>-$LysNH_2$

[a]*γ-gdm* = C*γ-gdm*, *β-gdm* = C*β-gdm*.

UV Melting Studies of *γ/β-gdm*-PNA: DNA Hybrids. The antiparallel and parallel duplexes with complementary DNA were obtained from *γ-gdm*-PNA oligomers (PNA **2**−PNA **5**) and C*β-gdm*-PNA oligomers (PNA **6**−PNA **9**) by stoichiometric mixing of each PNA oligomer with DNA **1** (antiparallel) and DNA **2** (parallel), respectively (Figure 3).

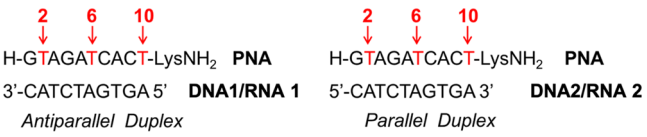

Figure 3. Relative orientations of PNA and DNA strand antiparallel and parallel duplexes. T represents *α-*, *β-*, and *γ-gdm*-PNA units.

The T_m of each duplex was determined by temperature-dependent changes in the UV absorbance[49−52] (UV-T plot), which exhibited typical sigmoidal behavior (Figure 4), suggesting the successful formation of duplexes in both parallel and antiparallel orientations. The thermal stabilities (T_m) of duplexes of all PNAs (PNA **1**−PNA **9**) with complementary antiparallel DNA **1** and parallel DNA **2** corresponding to the midpoint of biphasic transitions in UV−temperature plots (Figure 4) were obtained accurately from the maxima in their first derivative curves (Supporting Information) and are shown in Table 2.

***γ-gdm*-PNA:DNA Duplexes.** The unmodified antiparallel duplex *aeg*-PNA **1**:DNA **1** showed a T_m of 49.1 °C, and the T_m of *γ-gdm*-modified PNA:DNA duplexes showed a decrease as a function of the number and site of modifications (Figure 4A and Table 2). The destabilization of the duplexes compared to the unmodified PNA **1**:DNA **1** duplex was as follows: single substitution at the N-terminus (t^2, PNA **2**:DNA **1**) by 9.3 °C and substitution at the middle (t^6, PNA **3**:DNA **1**) by 7.3 °C, (Table 2, entries 2 and 3), double substitution ($t^{2,6}$, PNA **4**:DNA **1**) by 8.7 °C (Table 2, entry 4), and triple substitution ($t^{2,6,10}$, PNA **5**:DNA**1**) by 10.9 °C (Table 2, columns DNA **1**, entries 1−5).

In the case of parallel duplexes, (Figure 4B) the unmodified PNA **1**:DNA **2** duplex showed a T_m of 41.1 °C destabilized by 8 °C compared to that of its antiparallel duplex PNA **1**:DNA **1** as is known for PNA:DNA duplexes.[1] However, in contrast to the antiparallel duplexes, the C*γ-gdm*-substituted PNAs (PNA **2**−PNA **5**) actually enhanced the T_m of the derived parallel duplexes with DNA **2** compared to that of unsubstituted parallel duplex PNA **1**:DNA **2**. The stabilization increased as follows: N-terminus (t^2, PNA **2**:DNA **2**; +4.3 °C), middle (t^6, PNA **3**:DNA **2**; +1.9 °C), double ($t^{2,6}$, PNA **4**:DNA **2**; +5.0 °C), and triple ($t^{2,6,10}$, PNA **5**:DNA **2**; +7.2 °C) with enhancement in T_m amounting to ∼2.4 °C/modification (Table 2, columns DNA **2**).

***β-gdm*-PNA:DNA Duplexes.** The UV−thermal stability melting curves for *β-gdm* PNA:DNA antiparallel and parallel duplexes are shown in Figure 4C,D, respectively, with the corresponding T_m values given in Table 2 (entries 6−9, DNA **1** column). The data indicated that successive substitutions of the *β-gdm* unit into the PNA oligomer destabilized the antiparallel duplexes with DNA similar to that seen with the corresponding *γ-gdm* PNA oligomers. Surprisingly, maximum destabilization was seen with single middle substitution (t^6, PNA **7**:DNA **1**; −12.5 °C) compared to that at the N-terminus

https://doi.org/10.1021/acsomega.2c05873
ACS Omega 2022, 7, 40558−40568

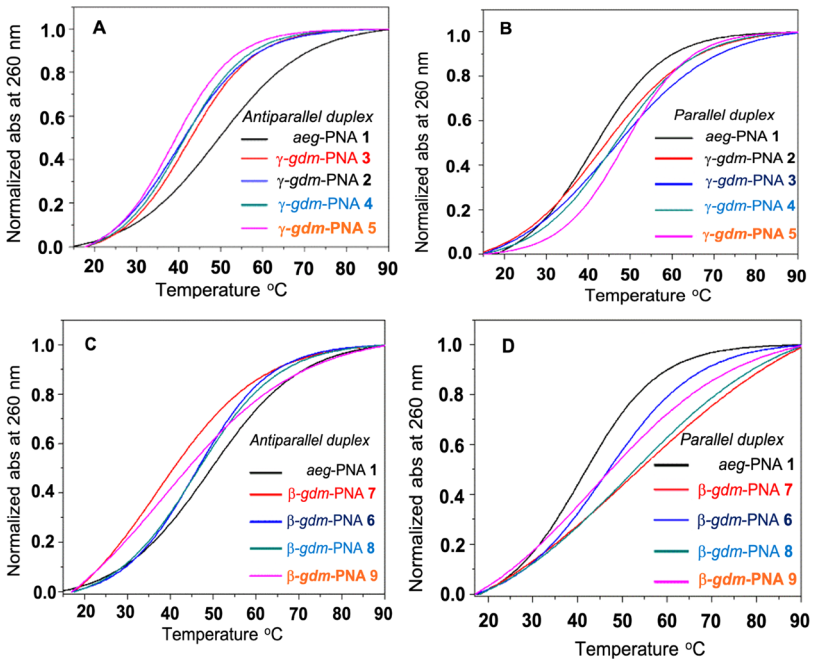

Figure 4. UV-T_m curves of (A) *γ-gdm*-PNA:DNA**1** antiparallel, (B) *γ-gdm*-PNA:DNA**2** parallel, (C) *β-gdm*-PNA:DNA**1** antiparallel, and (D) *β-gdm*-PNA:DNA**2** parallel duplexes. Buffer: 10 mM aq. sodium phosphate, pH 7.2, and NaCl: 10 mM.

Table 2. UV-T_m of *γ-gdm*-PNA:DNA/RNA Antiparallel and Parallel Duplexes[a]

		DNA 1 (*ap*)		DNA 2 (*p*)		RNA 1 (*ap*)		RNA 2 (*p*)	
entry	PNA code	T_m	ΔT_m	T_m	ΔT_m	T_m	ΔT_m	T_m	ΔT_m
1	*aeg* PNA **1**	49.1		41.1		52.1		39.4	
2	*γ-gdm*-t^2 PNA **2**	39.8	−9.3	45.4	+4.3	51.5	−0.6	41.4	+2.0
3	*γ-gdm*-t^6 PNA **3**	41.8	−7.3	43.0	+1.9	47.7	−4.4	40.5	+1.1
4	*γ-gdm*-$t^{2,6}$ PNA **4**	40.4	−8.7	46.1	+5.0	45.6	−6.5	40.0	+0.6
5	*γ-gdm*-$t^{2,6,10}$ PNA **5**	38.2	−10.9	48.3	+7.2	43.2	−8.9	38.2	−1.2
6	*β-gdm*-t^2 PNA **6**	46.1	−3.0	46.2	+5.1	49.1	−2.2	38.6	−0.8
7	*β-gdm* t^6 PNA **7**	36.6	−12.5	52.8	+11.7	33.5	−17.8	29.7	−9.7
8	*β-gdm*-$t^{2,6}$ PNA **8**	45.5	−3.6	51.9	+10.8	32.7	−19.4	40.5	+1.1
9	*β-gdm*-$t^{6,10}$ PNA **9**	38.6	−10.5	43.9	+2.8	40.1	−12.0	33.5	−5.9

[a]**DNA 1**/ **RNA 1** (*ap*, antiparallel), 3′-CATCTAGTGA-5′; **DNA 2**/**RNA 2** (*p*, parallel): 5′-CATCTAGTGA-3′; ΔT_m indicates the difference in T_m with control *aeg* PNA; T_m values are accurate to ±0.5 °C. + indicates stabilization; − indicates destabilization.

(t^2, PNA **6**:DNA **1**; −3.0 °C) and double modifications ($t^{2,6}$, PNA **8**:DNA **1**; −3.6 °C and $t^{6,10}$, PNA **9**:DNA **1**; −10.5 °C) (Table 2, entries 6−9, DNA columns). In contrast, the parallel *β-gdm* PNA:DNA **2** duplexes became stabilized with successive *β-gdm* substitutions at t^2 (PNA **6**:DNA **2**; +5.1 °C), t^6 (PNA **7**:DNA **2**; +11.7 °C), $t^{2,6}$ (PNA **8**:DNA **2**; +10.8 °C), and $t^{6,10}$ (PNA **9**:DNA **2**; +2.8 °C) compared to the unsubstituted PNA **1**:DNA **2** duplex (Table 2, entries 6−9, DNA **2** column).

The overall data in Table 2 indicate that while the antiparallel duplex is more stable than the parallel duplex in unsubstituted PNA, with both *γ*- and *β-gdm*-PNA:DNA duplexes, a reverse trend is observed: *the parallel duplexes are more stable than the analogous antiparallel duplexes*. This is a notable result on the effect of position-dependent *gdm* substitution in the *aeg*-PNA backbone.

UV Melting Studies of *γ*/*β-gdm*-PNA:RNA Hybrids. The comparative hybridization properties of *γ*/*β-gdm*-PNA with RNA **1** in the antiparallel orientation and RNA **2** in the parallel orientation (Table 2) were similarly examined by temperature-dependent UV absorbance (Figure 5). The sigmoidal behavior of UV-T plots typical of two-state transitions confirmed the formation of both parallel and antiparallel duplexes, and T_m values were obtained from the maxima in the first derivative plots (Supporting Information). Increasing the substitution of *γ-gdm* units destabilized the antiparallel duplexes with RNA **1** (Table 2, entries 2−5, RNA **1** column, −0.6 to −8.9 °C) compared to the unsubstituted *aeg*-PNA **1**:RNA **1** duplex (entry 1). However, the corresponding parallel duplexes *γ-gdm*-PNA: RNA **2** did not show much variation (Table 2, entries 2−5, −1.2 to +2.0 °C; RNA **2** column). The antiparallel *β-gdm*-PNA:RNA **1** duplexes exhibited destabilization compared to the unsubstituted PNA:RNA **1** duplex (Table 2, entries 6−9, −2.2 to −19.4 °C, RNA **1** column,), much more than that of the analogous *γ-gdm*-PNA:RNA **1** antiparallel duplexes (Table 2, entries 2−5, −0.6 to −8.9 °C, RNA **1** column). The corresponding parallel duplexes of *β-gdm*-PNA with RNA **2** (Table 2, entries 6−9, −9.7 to +1.1 °C, RNA **2** column) were destabilized to a greater degree compared to the more stable *γ-gdm*-PNA:RNA **2** duplexes (Table 2, entries 2−5, −1.2 to +2.0 °C, RNA **2** column). Thus, in the case of *γ*/*β-gdm* PNAs, the antiparallel duplexes with RNA **1** were significantly destabilized and the

https://doi.org/10.1021/acsomega.2c05873
ACS Omega 2022, 7, 40558−40568

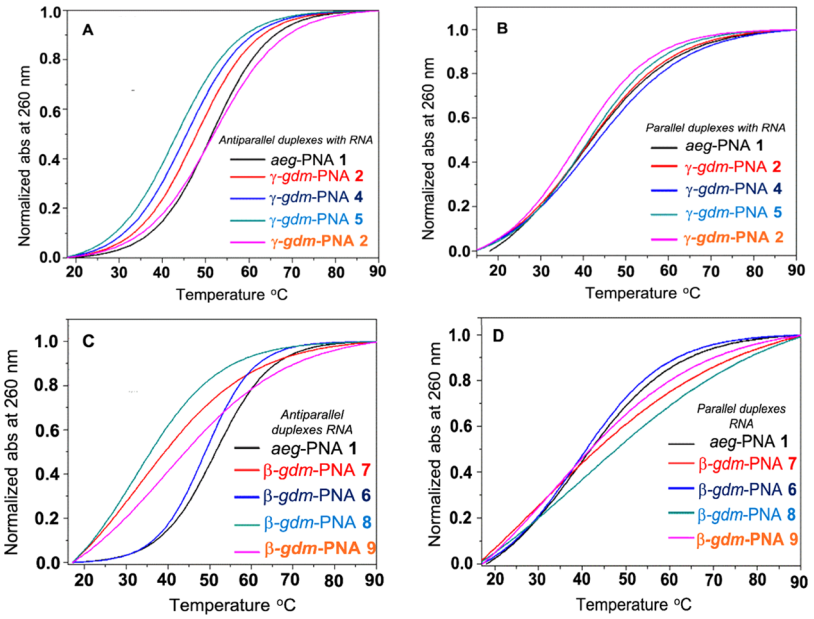

Figure 5. UV-T_m curves of (A) *γ-gdm*-PNA:RNA**1** antiparallel, (B) *γ-gdm*-PNA:RNA**2** parallel, (C) *β-gdm*-PNA:RNA**1** antiparallel, and (D) *β-gdm*-PNA:RNA**2** parallel duplexes. Buffer: 10 mM aq. sodium phosphate, pH 7.2, and NaCl: 10 mM.

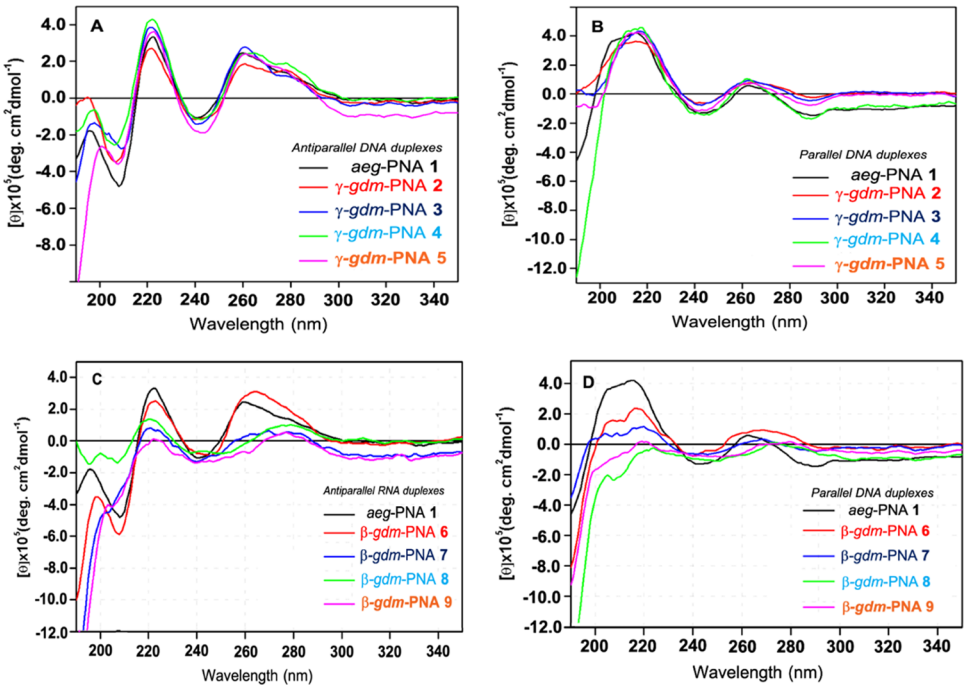

Figure 6. CD profiles of *γ/β-gdm*-PNA duplexes with DNA. *aeg*-PNA, γ^2, γ^6, $\gamma^{2,6}$, and $\gamma^{2,6,10}$—*gdm*-PNA, (A) antiparallel with DNA **1**, (B) *parallel* with DNA **2**; *aeg*-PNA, β^2, β^6, $\beta^{2,6}$, and $\beta^{6,10}$—*gdm*-PNA, (C) antiparallel with RNA **1**, and (D) parallel with RNA **2**. Buffer: 10 mM sodium cacodylate, pH 7.2, and NaCl: 10 mM.

equivalent parallel duplexes with RNA **2** were marginally destabilized compared to *aeg*-PNA:RNA duplexes. Overall, the *γ/β-gdm* PNA:RNA antiparallel duplexes were more stable than the parallel duplexes, which was the reverse of that seen for *γ/β-gdm* PNA:DNA duplexes. This clearly suggested the effect of the *gdm* substitutions on their relative hybridization stabilities with DNA and RNA, parallel DNA duplexes > antiparallel DNA duplexes and parallel RNA duplexes < antiparallel RNA duplexes (only for *β*).

CD Spectroscopic Studies of Antiparallel and Parallel *γ/β-gdm* PNA:DNA Duplexes. CD spectroscopy shows the characteristic spectra for different PNA:DNA/RNA duplexes.[53] Both *γ*- and *β-gdm* PNA:DNA antiparallel duplexes (Figure 6A/C) are characterized by major positive bands of comparable intensities at 220 and 260 nm, the latter band being broad with a shoulder at 275 nm. The negative bands are of high intensity at 210 nm, with weak to moderate intensity at 240 nm. In the case of *β-gdm* PNA:DNA antiparallel duplexes (Figure 6C), the band intensities are weak in monosubstituted oligomers and became prominent with disubstituted analogues. In comparison, all *γ-gdm* PNA:DNA parallel duplexes showed a high intensity positive band at 220 nm, followed by a much

https://doi.org/10.1021/acsomega.2c05873
ACS Omega 2022, 7, 40558−40568

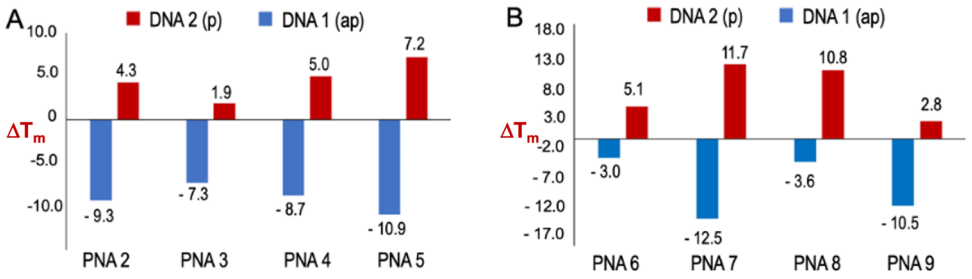

Figure 7. Comparative stabilities *γ*/*β*-*gdm*-PNA:DNA duplexes relative to *aeg*-PNA:DNA duplexes. Stabilization (red bars) and destabilization (blue bars) of antiparallel and parallel duplexes of (A) *γ*-*gdm*-PNA and (B) *β*-*gdm*-PNA with DNA **1** (*ap*) and DNA **2** (*p*). ΔT_m indicates T_m difference compared to T_m of *aeg*-PNA:DNA duplexes.

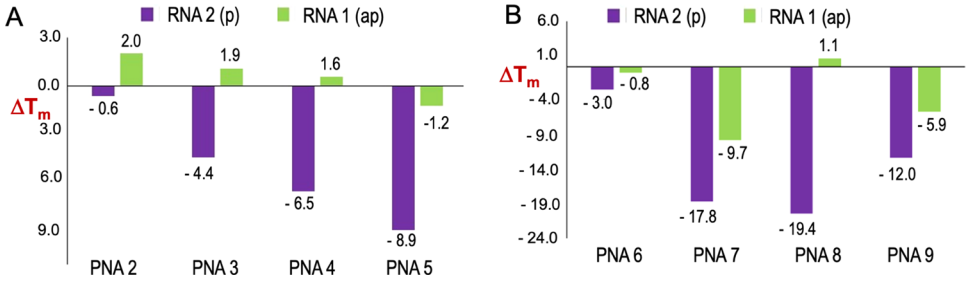

Figure 8. Comparative stabilities of *γ*/*β*-*gdm*-PNA:RNA duplexes relative to *aeg*-PNA:RNA duplexes. Stabilization (green bars) and destabilization (purple bars) of antiparallel and parallel duplexes of (A) *γ*-*gdm*-PNA and (B) *β*-*gdm*-PNA with RNA **1** (*ap*) and RNA **2** (*p*). ΔT_m indicates T_m difference compared to T_m of *aeg*-PNA:RNA duplexes.

weaker positive band at 260 nm, without much effects of the degree of substitution (Figure 6B). The broad positive shoulder at 280 nm seen in antiparallel duplexes is noticeably weaker or absent in parallel duplexes and replaced by a weak negative band (Figure 6B). A similar pattern is seen for parallel *β*-*gdm* duplexes, with the intensities of bands at 220 nm increasing in disubstituted oligomers (Figure 6D). While parallel (Figure 6B,D) and antiparallel (Figure 6A,C) duplexes show distinct differences in the CD profile among them, within each type, the CD profiles are similar to those of unsubstituted *aeg*-PNA:DNA duplexes. This indicates that no major conformational differences are induced by *γ*/*β*-*gdm* substitutions compared to analogous *aeg*-PNA duplexes.

Comparative Thermal Stabilities of *γ*-*gdm* and *β*-*gdm* PNA Duplexes with DNA and RNA. The temperature-dependent UV absorbance data (Table 2) showed variation in the thermal stabilities of *γ*/*β*-*gdm*-PNA:DNA antiparallel and parallel duplexes depending on the type and number of *gdm* modifications incorporated into PNA oligomers (Figure 7). As compared to the unmodified *aeg*-PNA:DNA duplexes, the *γ*/*β*-*gdm*-PNA:DNA parallel duplexes were stabilized (Figure 7, red bars) and antiparallel duplexes were destabilized (Figure 6, blue bars). Generally, *β*-*gdm*-PNA:DNA **1** parallel duplexes (Figure 7B) were more stable than *γ*-*gdm*-PNA:DNA **1** (Figure 7A), and the destabilization of antiparallel duplexes was dependent on the site of substitution, with *gdm*-PNAs having middle modifications being more destabilized.

In comparison, *γ*/*β*-*gdm*-PNA:RNA duplexes (Figure 8) exhibited low or negligible stabilization of *γ*-*gdm*-PNA:RNA antiparallel duplexes (ΔT_m, < 2.0 °C) decreasing with increasing substitution, while *γ*-*gdm*-PNA:RNA parallel duplexes became significantly destabilized compared to *aeg*-PNA:RNA duplex (Figure 8A). The *β*-*gdm*-PNA:RNA duplexes uniformly showed significant destabilization of both parallel and antiparallel duplexes relative to that of analogous *aeg*:PNA:RNA duplexes (Figure 8B). Inspite of destabilization with respect to unsubstituted *aeg*-PNA:RNA duplexes, the *γ*/*β*-*gdm*-PNA:RNA antiparallel duplexes showed higher stability than that of parallel duplexes, a reverse trend of that seen in *γ*/*β*-*gdm*-PNA:DNA duplexes. In contrast, *α*-*gdm*-PNAs showed an opposite preference of binding to RNA rather than to DNA.[34] The triple-modified identical sequence H-G**t**AGA**t**-CAC**t**-LysNH$_2$ (**t** = *α*-*gdm*) stabilized the antiparallel DNA duplex over the parallel duplex by 24.4 °C and antiparallel RNA duplex over the parallel duplex by 40.0 °C.[34] The *α*-*gdm*-PNA:RNA duplex had higher stability than that of the *α*-*gdm*-PNA:DNA duplex by 3.0 °C for the parallel orientation, while it was almost similar for the antiparallel duplex.

DISCUSSION

The achiral *α*/*β*/*γ*-*gdm*-dimethyl groups in *gdm*-PNAs introduce steric rigidity into the somewhat conformationally flexible *aeg*-backbone of PNA. The nature and extent of conformational constrains in the *gdm*-backbone and its effects on the stability of duplexes with DNA/RNA are clearly dependent on the *α*/*β*/*γ*-site of substitution. The *α*-*gdm*-PNA with achiral gemdimethyl substitution on C*α* in the glycine segment stabilized the derived (homo-PNA-T$_n$)$_2$:(homo-A$_n$-DNA/RNA) triplexes compared to the unsubstituted *aeg*-PNA triplexes. The mixed-base PNA sequence incorporating *α*-*gdm*-T substitutions stabilized the resulting *α*-*gdm*-PNA:DNA/RNA duplexes[36] compared to that with isosequential DNA/RNA, with the antiparallel duplexes exhibiting higher T$_m$ values than those of aeg-PNA duplexes. In comparison, the *β*/*γ*-*gdm* PNAs reported here exhibited an interesting trend of (i) parallel DNA and RNA duplexes being more stable than *aeg*-PNA:DNA/RNA duplexes, (ii) T_m of the parallel DNA duplexes higher than T_m of antiparallel DNA duplexes, (iii) T_m of antiparallel RNA duplexes higher than that of parallel RNA duplexes, (iv) for antiparallel duplexes, RNA duplexes

https://doi.org/10.1021/acsomega.2c05873
ACS Omega 2022, 7, 40558−40568

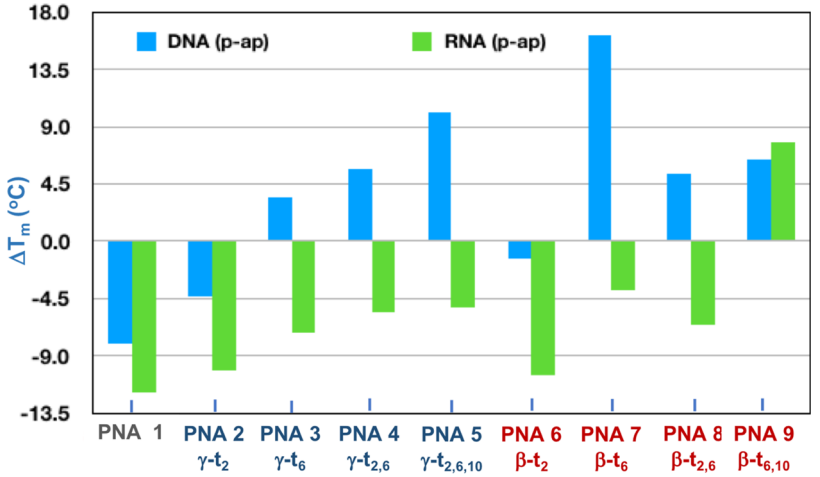

Figure 9. Comparative thermal stabilities of parallel/antiparallel DNA/RNA duplexes of *γ-gdm* and *β-gdm*-PNA.

with higher melting than that of DNA duplexes, and (v) for parallel duplexes, DNA duplexes with higher melting than that of RNA duplexes. The relative preferences in the binding of *α/β/γ-gdm*-PNAs with DNA/RNA and in the parallel/antiparallel fashion may arise from the conformational preorganization of the PNA backbone to assume a favorable hybridization-competent conformation. An interesting attribute seen in *α-gdm*-PNA and *β-gdm*-PNA oligomers is that the former stabilizes the DNA duplex in the antiparallel orientation,[34] while the latter stabilizes DNA duplexes in the parallel orientation.

The conformational constrain in *α/β/γ-gdm*-PNA is caused briefly by the Thorpe−Ingold effect[54] exerted by gemdimethyl groups, which may alter the backbone dihedral angles and thereby influence the PNA E/Z-rotamer population. The combined steric and electronic factors vary with the site of substitution, inducing different conformational stabilities of E/Z-rotamers as experimentally observed by us in ^{1}H NMR of *α-*, *β-*, and *γ-gdm*-PNA-T monomers and by computational results.[39] The *β-gdm*-PNA-T monomer shows exclusively E-rotamers in solution, while the *γ-gdm*-PNA-T monomer crystallized as E-rotamers (Figure 2). In crystal structures with the base-modified cyanuryl *aeg*-PNA monomer[55] and in *α*-mono- or *β/γ*-disubstituted cyclic *aeg*-PNAs,[56,57] the Z-rotamer has been exclusively observed. The major Z-rotamer seen for *aeg*-PNA at the monomer level leads to antiparallel PNA duplexes containing exclusively the Z-rotamer.[41−43] Hence, if the exclusively seen E-rotamer for the *β-gdm*-PNA monomer also prevails in the corresponding PNA:DNA oligomers that show higher stability parallel duplexes, it is tempting to suggest that the E-rotamer may lead to preferential parallel duplexes, while the Z-rotamer results in antiparallel duplexes. Further structural and computational studies are needed at the oligomer level to verify the existence of such a correlation. It is relevant to point out that in olefinic OPA-PNA in which the tertiary amide group is replaced by C=C that restricts the structure to the E-type isomer, the parallel duplex is more stable than the antiparallel duplex.[58] The observed higher stability of parallel duplexes of the mixed sequence over that of antiparallel duplexes in *β/γ-gdm* PNAs is so far unusual in the PNA literature.

A comprehensive comparison of the relative thermal stabilities ΔT_m ($T_m p - T_m ap$) of parallel/antiparallel DNA/RNA duplexes of *γ-gdm* and *β-gdm*-PNA is depicted in Figure 9. In general, the results indicate that with *γ-* and *β-gdm* PNAs, (i) DNA parallel duplexes are more stable than antiparallel duplexes [blue bars, +(p-ap)], (ii) RNA antiparallel duplexes show higher stability compared to that of DNA duplexes [green bars, -(p-ap)], and (iii) increased substitutions enhance parallel duplex stability. As established in the literature, modifications in the center of the sequences exert maximum destabilization effects, which follows the order $t^6 > t^{2,6} > t^{10} > t^{6,10}$. The CD spectral profiles clearly show difference between parallel and antiparallel duplexes and confirm the thermal stability results.

CONCLUSIONS

We have demonstrated that the introduction of appropriate rigidity in the form of gemdimethyl substitution into the *aeg* backbone of PNA without imparting chirality improves not only the DNA/RNA binding properties of PNA but also its selectivity for DNA and prime preference for parallel duplex formation. The results presented here complement our earlier work that had demonstrated that chiral cyclohexanyl-PNAs favor binding with RNA compared with DNA[18] and *α-gdm*-PNAs showing reversed preference for binding DNA to RNA.[34] Although true validation should be derived from completely modified oligomers, significant selectivity is seen even in the partially substituted *gdm*-PNA oligomers. The present work advances the concept of engineering affinity and selectivity in PNA:DNA/RNA binding by structural tuning of the gemdimethyl substitution site on the backbone to yield specific Z- or E-rotamers. Such structural consequences of the sterically rigid achiral gemdimethyl groups in preorganizing the backbone conformation are favorable for complexation with DNA or RNA. The simple achiral gemdimethyl substitution to tune the PNA rotamer formation adds a new repertoire to the arsenal of PNA modifications. Recently, di-guaninyl PNA has attracted attention in terms of unusual light emitting properties due to a combination of base stacking and H-bonding interactions,[59] facilitated by the Z-rotamer. It would be interesting to study such structure−light emitting property interactions induced by the E-rotamer through gemdimethyl substitutions, which may change the base stacking interactions. One can also extend the concept by simultaneous introduction of gemdimethyl substitutions at two sites on the backbone or structurally combining with the recently reported bimodal PNAs.[60−63] The possibility of generating parallel duplexes with

https://doi.org/10.1021/acsomega.2c05873
ACS Omega 2022, 7, 40558−40568

selectivity for DNA or RNA may also lead to novel platforms for biomolecular engineering of PNA, affording novel nano-assemblies.[64−68] The introduction of gemdimethyl substituents also changes the overall hydrophobicity of PNA oligomers, thereby influencing their cell penetration properties, and may lead to newer motifs for molecular assemblies in biomedical applications,[69−71] in view of the well-documented physico-chemical, structural, and biological properties imparted by *gem*-dimethyl groups in medicinal chemistry.[72]

EXPERIMENTAL SECTION

The *aeg*-PNA, *β-gdm*-PNA-T, and *γ-gdm*-PNA-T monomers were synthesized by previously reported procedures[34,39] and used for solid-phase synthesis.[46] Mass spectra were obtained using an Applied Biosystems 4800 Plus MALDI-TOF/TOF mass spectrometer using TiO_2 or 2,5-dihydroxybencoic acid (DHB), and the integrity of the PNA oligomer was checked on the same instrument using DHB or CHCA as the matrix. High-resolution mass spectra for final PNA monomers were recorded on a Synapt G2 high-definition mass spectrometer.

Synthesis of PNA Oligomers by Solid-Phase PNA Synthesis. The *aeg*-PNA monomers and *γ/β-gdm*-PNA-T monomers were incorporated into the 10-mer PNA oligomer sequence H-GTAGATCACT-LysNH_2 using standard solid-phase protocol on L-lysine-derivatized MBHA resin.[60] The amine content on the resin was suitably lowered from 2 mmol/g to 0.35 mmol/g by partial acylation of amino groups using a calculated amount of acetic anhydride. The desired PNA monomers were coupled sequentially to assemble the PNA sequence using PyBOP and DIPEA in DMF/NMP as coupling reagents. The PNA oligomers were synthesized using repetitive cycles, each comprising the following steps: (i) deprotection of the *N-t*-Boc group using 50% TFA in DCM (3 × 15 min), (ii) washing of beads with DCM, DMF, and again DCM (thrice each), (iii) neutralization of the TFA salt of amine using 10% DIPEA in DCM to liberate free amine (3 × 10 min), (iv) washing of beads with DCM and DMF (thrice with each solvent), and (v) coupling of the free amine with activated carboxyl of the incoming monomer (3 equiv) using coupling agents. The coupling reactions were carried out in DMF/NMP with PyBOP as coupling reagents in the presence of DIPEA. Capping (when needed) of the unreacted amino groups was done using Ac_2O in pyridine:DCM. After each coupling and deprotection step, Kaiser's test[47,48] was done for the confirmation of PNA chain elongation using the following reagents: (a) ninhydrin (5.0 g) dissolved in ethanol (100 mL), (b) phenol (80.0 mg) dissolved in ethanol (20 mL), and (c) potassium cyanide (2 mL, 0.001 M aq. solution) in pyridine (98 mL). After every coupling, few resin beads were taken in a test tube, washed with ethanol and 3−4 drops of each of the above-mentioned solutions were added. The test tube was heated for 1−2 min, and the emergence of color indicated the free uncoupled amine on the resin. In such a case, the coupling was continued with a second addition to complete the reaction.

Cleavage of the PNA Oligomers from the Solid Support. The MBHA resin (10 mg) carrying the synthesized PNA oligomers was stirred with thioanisole (20 μL) and 1,2-ethanedithiol (8 μL) in an ice bath for 10 min. TFA (200 μL) was added under cooling and kept in an ice bath. TFMSA (16 μL) was added slowly with stirring to dissipate the generated heat. The reaction mixture was stirred for 1.5−2 h at room temperature. The resin was removed by filtration under reduced pressure and washed twice with TFA. The filtrate was combined and evaporated on a rotary evaporator at ambient temperature. The residue was transferred to an Eppendorf tube, and the peptide was precipitated by trituration with cold dry ether. The peptide was isolated by centrifugation, and the precipitate was dissolved in deionized water and used for purification.

Purification of the PNA Oligomers by RP-HPLC. PNA oligomers were purified on an Agilent HPLC system using a semipreparative BEH130 C18 (10 mm × 250 mm) column. The elution was done using water and CH_3CN employing gradient elution: solvent A = 0.1% TFA in CH3CN:H2O (5:95); solvent B = 0.1% TFA in CH3CN:H2O (1:1), A to 100% B in 45 min; and flow rate of 3 mL/min with monitoring of eluants at 254 nm.

Temperature−UV Absorbance Measurements. UV melting experiments were carried out on a Varian Cary 300 UV spectrophotometer equipped with a Peltier heating system. The samples were prepared in sodium cacodylate buffer (10 mM) and NaCl (10 mM); pH 7.2. Individual PNA oligomers and complementary DNA/RNA were mixed in a stoichiometric ratio (1:1, duplex) to achieve a final concentration of 2 μM for each strand. The samples were annealed by heating the mixture at 90 °C for 10 min and cooled slowly to room temperature over 8−10 h, followed by refrigeration for 24 h. The samples (500 μL) were transferred to a quartz cell and equilibrated at room temperature for 5 min. The absorbance at 260 nm was recorded in steps from 20 to 90 °C with a temperature increase of 0.5 °C. The absorbance plotted at 260 nm as a function of the temperature was fitted by a sigmoidal curve, with the *R* square value in range of 0.96−0.99. The data were processed using OriginPro 8.5. The T_m was determined from the first derivative of normalized absorbance with respect to the temperature and is accurate to ±1.0 °C. Each melting experiment was repeated thrice. The concentrations of all oligonucleotides were calculated on the basis of absorbance at 260 nm from the molar extinction coefficients of the corresponding nucleobases: T = 8.8 $cm^2/\mu mol$; C = 6.6 $cm^2/\mu mol$; G = 11.7 $cm^2/\mu mol$, and A = 13.7 $cm^2/\mu mol$ as per the literature.[49]

Circular Dichroic Spectra. CD spectra were recorded on a JASCO J-815 spectropolarimeter. The PNA:DNA samples were prepared by stoichiometric mixing and annealing in the same way as for UV spectral studies. The CD spectra of *bm*-PNA:DNA complexes were recorded with samples in a 2 mm cell at a temperature of 10 °C, scanning from 300 to 200 nm using a resolution of 0.1 nm, bandwidth of 1 nm, sensitivity of 2 mdeg, response of 2 s, and scan speed of 50 nm/min. Final spectra are shown as the addition of three scans.

ASSOCIATED CONTENT

Supporting Information

The Supporting Information is available free of charge at https://pubs.acs.org/doi/10.1021/acsomega.2c05873.

HPLC and MALDI-TOF spectral data of all PNA oligomers and UV-T plots (sigmoidal and first derivative) of *γ-dmg* PNA:DNA, *γ-dmg* PNA:RNA, *β-dmg* PNA:DNA, and *β-dmg* PNA:RNA duplexes (PDF)

AUTHOR INFORMATION

Corresponding Author

Krishna N. Ganesh − *Indian Institute of Science Education and Research (IISER) Pune, Pune 411008, India;*

https://doi.org/10.1021/acsomega.2c05873
ACS Omega 2022, 7, 40558−40568

orcid.org/0000-0003-2292-643X; Email: kn.ganesh@iisertirupati.ac.in

Authors

Pradnya Kulkarni − *Chemistry Department, Indian Institute of Science Education and Research (IISER) Tirupati, Tirupati 517507, India*

Dhrubajyoti Datta − *Chemistry Department, Indian Institute of Science Education and Research (IISER) Tirupati, Tirupati 517507, India;* Present Address: 675 West Kendall Street Alnylam Pharmaceuticals Inc., Boston, USA, ddatta@alnylam.com

Complete contact information is available at: https://pubs.acs.org/10.1021/acsomega.2c05873

Notes

The authors declare no competing financial interest.

■ ACKNOWLEDGMENTS

P.K. acknowledges the award of the research fellowship from the CSIR (New Delhi). D.D. thanks IISER Pune for award of a post-doctoral research fellowship.

■ REFERENCES

(1) Nielsen, P. E.; Egholm, M.; Berg, R. H.; Buchardt, O. Sequence-selective recognition of DNA by strand displacement with a thymine-substituted polyamide. *Science* **1991**, *254*, 1497−1500.

(2) Egholm, M.; Buchardt, O.; Christensen, L.; Behrens, C.; Freier, S. M.; Driver, D. A.; Berg, R. H.; Kim, S. K.; Norden, B.; Nielsen, P. E. PNA hybridizes to complementary oligonucleotides obeying the Watson-Crick hydrogen-bonding rules. *Nature* **1993**, *365*, 566−568.

(3) Egholm, M.; Buchardt, O.; Nielsen, P. E.; Berg, R. H. Peptide nucleic acids (PNA): Oligonucleotide analogs with an achiral peptide backbone. *J. Am. Chem. Soc.* **1992**, *114*, 1895−1897.

(4) Egholm, M.; Nielsen, P. E.; Buchardt, O.; Berg, R. H. Recognition of guanine and adenine in DNA by cytosine and thymine containing peptide nucleic acids (PNA). *J. Am. Chem. Soc.* **1992**, *114*, 9677−9678.

(5) Egholm, M.; Buchardt, O.; Christensen, L.; Behrens, C.; Freier, S. M.; Driver, D. A.; Berg, R. H.; Kim, S. K.; Norden, B.; Nielsen, P. E. PNA hybridizes to complementary oligonucleotides obeying the Watson−Crick hydrogen-bonding rules. *Nature* **1993**, *365*, 566−568.

(6) Nielsen, P. E. Peptide Nucleic Acid: A molecule with two Identities. *Acc. Chem. Res.* **1999**, *32*, 624−630.

(7) Ray, A.; Nordén, B. Peptide nucleic acid (PNA): its medical and biotechnical applications and promise for the future. *FASEB. J.* **2000**, *14*, 1041−1060.

(8) Nielsen, P. E. PNA Technology. *Mol. Biotechnol.* **2004**, *26*, 233−248.

(9) Lundin, K. E.; Good, L.; Strömberg, R.; Gräslund, A.; Smith, C. I. E.Biological activity and biotechnological aspects of peptide nucleic acid. In *Advances in Genetics*; Academic Press, 2006; Vol. *56*, pp 1−51, DOI: 10.1016/S0065-2660(06)56001-8.

(10) D'Agata, R.; Giuffrida, M. C.; Spoto, G. Peptide nucleic acid based biosensors for cancer diagnosis. *Molecules* **2017**, *22*, 1951−1966.

(11) Vilaivan, T. Fluorogenic PNA probes. *Beilstein J. Org. Chem.* **2018**, *14*, 253−281.

(12) Montazersaheb, S.; Hejazi, M. S.; Nozad Charoudeh, H. Potential of peptide nucleic acids in future therapeutic applications. *Adv. Pharm. Bull.* **2018**, *8*, 551−563.

(13) Saarbach, J.; Sabale, P. M.; Winssinger, N. Peptide nucleic acid (PNA) and its applications in chemical biology, diagnostics, and therapeutics. *Curr. Opin. Chem. Biol.* **2019**, *52*, 112−124.

(14) Economos, N. G.; Oyaghire, S.; Quijano, E.; Ricciardi, A. S.; Saltzman, W. M.; Glazer, P. M. Peptide nucleic acids and gene editing: Perspectives on structure and repair. *Molecules* **2020**, *25*, 735−756.

(15) Hyrup, B.; Egholm, M.; Nielsen, P. E.; Wittung, P.; Norden, B.; Buchardt, O. Structure-activity studies of the binding of modified peptide nucleic acids (PNAs) to DNA. *J. Am. Chem. Soc.* **1994**, *116*, 7964−7970.

(16) Kumar, V. A.; Ganesh, K. N. Conformationally Constrained PNA Analogues: Structural Evolution toward DNA/RNA Binding Selectivity. *Acc. Chem. Res.* **2005**, *38*, 404−412.

(17) Govindaraju, T.; Kumar, V. A.; Ganesh, K. N. (1*S*,2*R*/1*R*,2*S*)-*cis*-Cyclopentyl PNAs (cpPNAs) as constrained PNA analogues: Synthesis and evaluation of *aeg*-cpPNA chimera and stereopreferences in hybridization with DNA/RNA. *J. Org. Chem.* **2004**, *69*, 5725−5734.

(18) Govindaraju, T.; Kumar, V. A.; Ganesh, K. N. (*SR*/*RS*)-Cyclohexanyl PNAs: Conformationally Preorganized PNA Analogues with Unprecedented Preference for Duplex Formation with RNA. *J. Am. Chem. Soc.* **2005**, *127*, 4144−4145.

(19) Kumar, V. A.; Ganesh, K. N. Structure-editing of nucleic acids for selective targeting of RNA. *Curr. Top. Med. Chem.* **2007**, *7*, 715−726.

(20) Mitra, R.; Ganesh, K. N. Aminomethylene peptide nucleic acid (*am*-PNA): Synthesis, regio-/stereospecific DNA binding, and differential cell uptake of (α/γ,R/S)-*am*-PNA analogues. *J. Org. Chem.* **2012**, *77*, 5696−5704.

(21) Jain, D. R.; Anandi, L. V.; Lahiri, M.; Ganesh, K. N. Influence of pendant chiral C^{γ}-(alkylideneamino/guanidino) cationic sidechains of PNA backbone on hybridization with complementary DNA/RNA and cell permeability. *J. Org. Chem.* **2014**, *79*, 9567−9577.

(22) Ellipilli, S.; Palvai, S.; Ganesh, K. N. Fluorinated Peptide Nucleic Acids with Fluoroacetyl side chain bearing 5-(F/CF_3)-uracil: Synthesis and cell uptake studies. *J. Org. Chem.* **2016**, *81*, 6364−6373.

(23) Dragulescu-Andrasi, A.; Rapireddy, S.; Frezza, B. M.; Gayathri, C.; Gil, R. R.; Ly, D. H. A simple γ-backbone modification preorganizes peptide nucleic acid into a helical structure. *J. Am. Chem. Soc.* **2006**, *128*, 10258−10267.

(24) Ishizuka, T.; Yoshida, J.; Yamamoto, Y.; Sumaoka, J.; Tedeschi, T.; Corradini, R.; Sforza, S.; Komiyama, M. Chiral introduction of positive charges to PNA for double-duplex invasion to versatile sequences. *Nucleic Acids Res.* **2008**, *36*, 1464−1471.

(25) Corradini, R.; Sforza, S.; Tedeschi, T.; Totsingan, F.; Manicardi, A.; Marchelli, R. Peptide nucleic acids with a structurally biased backbone: Updated review and emerging challenges. *Curr. Top. Med. Chem.* **2011**, *11*, 1535−1554.

(26) Moccia, M.; Adamo, M. F.; Saviano, M. Insights on chiral, backbone modified peptide nucleic acids: Properties and biological activity. *Artif. DNA PNA XNA* **2014**, *5*, No. e1107176.

(27) Gambari, R. Peptide Nucleic Acids: a review on recent patents and technology transfer. *Expert Opin. Ther. Pat.* **2014**, *24*, 267−294.

(28) Pansuwan, H.; Ditmangklo, B.; Vilaivan, C.; Jiangchareon, B.; Pan-In, P.; Wanichwecharungruang, S.; Palaga, T.; Nuanyai, T.; Suparpprom, C.; Vilaivan, T. Hydrophilic and cell-penetrable pyrrolidinyl peptide nucleic acid via post-synthetic modification with hydrophilic side chains. *Bioconjugate Chem.* **2017**, *28*, 2284−2292.

(29) Zheng, H.; Botos, I.; Victor Clausse, V.; Nikolayevskiy, H.; Rastede, E. H.; Fouz, M. F.; Mazur, S. J.; Appella, D. H. Conformational constraints of cyclopentane peptide nucleic acids facilitate tunable binding to DNA. *Nucl. Acids Res.* **2021**, *49*, 713−725.

(30) Suparpprom, C.; Vilaivan, T. Perspectives on conformationally constrained peptide nucleic acid (PNA): insights into the structural design, properties and applications. *RSC Chem. Biol.* **2022**, *3*, 648−697.

(31) Brown, S. C.; Thomson, S. A.; Veal, J. M.; Davis, D. G. NMR solution structure of a peptide nucleic acid complexed with RNA. *Science* **1994**, *265*, 777−781.

(32) Brodyagin, N.; Katkevics, M.; Kotikam, V.; Ryan, C. A.; Rozners, R. Chemical approaches to discover the full potential of

peptide nucleic acids in biomedical applications. *Beilstein J. Org. Chem.* **2021**, *17*, 1641−1688.
(33) Karle, I. L.; Balaram, P. Structural characteristics of alpha-helical peptide molecules containing Aib residues. *Biochemistry* **1990**, *29*, 6747−6756.
(34) Gourishankar, A.; Ganesh, K. N. (*α*,*α*-dimethyl)glycyl (*dmg*) PNAs: achiral PNA analogs that form stronger hybrids with cDNA relative to isosequential RNA. *Artific. DNA, PNA, XNA.* **2012**, *3*, 5−13.
(35) Dueholm, K. L.; Egholm, M.; Behrens, C.; Christensen, L.; Hansen, H. F.; Vulpius, T.; Petersen, K. H.; Berg, R. H.; Nielsen, P. E.; Buchardt, O. Synthesis of peptide nucleic acid monomers containing the four natural nucleobases: thymine, cytosine, adenine, and guanine and their oligomerization. *J. Org. Chem.* **1994**, *59*, 5767−5772.
(36) Chen, S.-M.; Mohan, V.; Kiely, J. S.; Griffith, M. C.; Griffey, R. H. Molecular dynamics and NMR studies of single-stranded PNAs. *Tetrahedron Lett.* **1994**, *35*, 5105−5108.
(37) Oleszczuk, M.; Rodziewicz-Motowid, S.; B Falkiewicz, B. Restricted rotation in chiral peptide nucleic acid (PNA) monomers - influence of substituents studied by means of ^{1}H NMR. *Nucleos, Nucleotid, Nucleic Acids* **2001**, *20*, 1399−1404.
(38) Ovadia, R.; A -L Lebrunb, A. -L.; Barvikd, I.; Vasseure, J. J.; C Baragueyc, C.; Alvarez, A. Synthesis and structural characterization of monomeric and dimeric Peptide nucleic acid prepared by microwave-promoted multicomponent reaction. *Org. Biomol. Chem.* **2015**, *13*, 11052−11058.
(39) Kulkarni, P.; Datta, D.; Ramabhadran, R. O.; Ganesh, K. Gem-dimethyl peptide nucleic acid (*α*/*β*/*γ*-*gdm*-PNA) monomers: synthesis and the role of *gdm*-substituents in preferential stabilisation of Z/E-rotamers. *Org. Biomol. Chem.* **2021**, *19*, 6534−6545.
(40) Betts, L.; Josey, J. A.; Veal, J. M.; Jordan, S. R. Nucleic acid triple helix formed by a peptide nucleic acid-DNA Complex. *Science* **1995**, *270*, 1838−1842.
(41) Menchise, V.; De Simone, G.; Tedeschi, T.; Corradini, R.; Sforza, S.; Marchelli, R.; Capasso, D.; Saviano, M.; Pedone, C. Insights into peptide nucleic acid (PNA) structural features: The crystal structure of a D-lysine-based chiral PNA−DNA duplex. *Proc. Natl. Acad. Sci. U.S.A.* **2003**, *100*, 12021−12026.
(42) Yeh, J. I.; Shivachev, B.; Rapireddy, S.; Crawford, M. J.; Gil, R. R.; Du, S.; Madrid, M.; Ly, D. H. Crystal Structure of chiral *γ*−PNA with complementary DNA strand: Insights into the stability and specificity of recognition and conformational preorganization. *J. Am. Chem. Soc.* **2010**, *132*, 10717−10725.
(43) Kiliszek, A.; Banaszak, K.; Dauter, Z.; Rypniewski, W. The first crystal structures of RNA−PNA duplexes and a PNA-PNA duplex containing mismatches−−toward antisense therapy against TREDs. *Nucleic Acids Res.* **2016**, *44*, 1937−1945.
(44) Sugiyama, T.; Imamura, Y.; Demizu, Y.; Kurihara, M.; Takano, M.; Kittaka, A. *β*-PNA: Peptide nucleic acid (PNA) with a chiral center at the *β*-position of the PNA backbone. *Bioorg. Med. Chem. Lett.* **2011**, *21*, 7317−7320.
(45) Bose, T.; Banerjee, A.; Nahar, S.; Maiti, S.; Kumar, V. A. *β*,*γ*-Bis-substituted PNA with configurational and conformational switch: preferred binding to cDNA/RNA and cell-uptake studies. *Chem. Commun.* **2015**, *51*, 7693−7696.
(46) *Peptide Nucleic Acids Protocols and Applications*, 2nd ed.; Nielsen, P. E., Ed.; Horizon Bioscience: Norfolk, U.K., 2004.
(47) Kaiser, E.; Colescott, R. L.; Bossinger, C. D.; Cook, P. I. Color test for detection of free terminal amino groups in the solid-phase synthesis of peptides. *Anal. Biochem.* **1970**, *34*, 595−598.
(48) Sarin, V. K.; Kent, S. B. H.; Tam, J. P.; Merrifield, R. B. Quantitative monitoring of solid-phase peptide synthesis by the ninhydrin reaction. *Anal. Biochem.* **1981**, *117*, 147−157.
(49) Bentin, T.; Hansen, G. I.; Nielsen, P. E.Measurement of PNA binding to double-stranded DNA. In *Methods in Molecular Biology*; Nielsen, P. E., Ed.; Humana Press: Totowa, NJ, 2002; Vol. *208*, pp 91−109.
(50) Mergny, J.-L.; Lacroix, L. Analysis of thermal melting curves. *Oligonucleotides* **2003**, *13*, 515−537.
(51) Krupnik, O. V.; Guscho, Y. A.; Sluchanko, K. A.; Nielsen, P. E.; Lazurkin, Y. S. Thermodynamics of the melting of PNA_2/DNA triple helices. *J. Biomol. Struct. Dyn.* **2001**, *19*, 535−542.
(52) Jasiński, M.; Miszkiewicz, J.; Feig, M.; Trylska, J. Thermal Stability of Peptide Nucleic Acid Complexes. *J. Phys. Chem. B* **2019**, *123*, 8168−8177.
(53) Corradini, R.; Tedeschi, T.; Sforza, S.; Marchelli, R.Electronic Circular Dichroism of Peptide Nucleic Acids and Their Analogues. In *Comprehensive Chiroptical Spectroscopy: Applications in Stereochemical Analysis of Synthetic Compounds, Natural Products, and Biomolecules*; Berova, N.; Polavarapu, P. L.; Nakanishi, K.; Woody, R. W., Eds.; John Wiley & Sons, Inc., 2012; Vol. *2*, pp 581−617.
(54) Corradini, R.; Tedeschi, T.; Sforza, S.; Marchelli, R.; Toniolo, C.; Crisma, M.; Formaggio, F.; Peggion, C. Control of peptide conformation by the Thorpe-Ingold effect (C*α*-tetrasubstitution). *Pept. Sci.* **2001**, *60*, 396−419.
(55) Sanjayan, G. J.; Pedireddi, V. R.; Ganesh, K. N. Cyanuryl-PNA Monomer: Synthesis and Crystal Structure. *Org. Lett.* **2000**, *2*, 2825−2828.
(56) Govindaraju, T.; Gonnade, R. G.; Bhadbhade, M. M.; Kumar, V. A.; Ganesh, K. N. (1S,2R/1R,2S)-Aminocyclohexyl glycyl thymine PNA: Synthesis, Monomer Crystal Structures, and DNA/RNA Hybridization Studies. *Org. Lett.* **2003**, *5*, 3013−3016.
(57) Govindaraju, T.; Kumar, V. A.; Ganesh, K. N. *cis*-Cyclopentyl PNA (cpPNA) as constrained chiral PNA analogues: stereochemical dependence of DNA/RNA hybridization. *Chem. Commun.* **2004**, 860−861.
(58) Hollenstein, M.; Leumann, C. J. Synthesis and Incorporation into PNA of Fluorinated Olefinic PNA (F-OPA) Monomers. *Org. Lett.* **2003**, *5*, 1987−1990.
(59) Berger, O.; Adler-Abramovich, L.; Levy-Sakin, M.; Grunwald, A.; Liebes-Peer, Y.; Bachar, M.; Buzhansky, L.; Mossou, E.; Forsyth, V. T.; Schwartz, T.; Ebenstein, Y.; Frolow, F.; Shimon, L. J. W.; Patolsky, F.; Gazit, E. Light-emitting self-assembled peptide nucleic acids exhibit both stacking interactions and Watson−Crick base pairing. *Nat. Nanotechnol.* **2015**, *10*, 353−360.
(60) Gupta, M. K.; Madhanagopal, B. R.; Datta, D.; Ganesh, K. N. Structural design and synthesis of bimodal PNA that simultaneously binds two complementary DNAs to form fused double duplexes. *Org. Lett.* **2020**, *22*, 5255−5260.
(61) Bhingardeve, P.; Madhanagopal, B. R.; Ganesh, K. N. C*γ*(S/R)-Bimodal peptide nucleic acids (C*γ*-bm-PNA) form coupled double duplexes by synchronous binding to two complementary DNA strands. *J. Org. Chem.* **2020**, *85*, 13680−13693.
(62) Gupta, M. K.; Madhanagopal, B. R.; Ganesh, K. N. Peptide nucleic acid with double face: Homothymine−homocytosine bimodal C*α*-PNA (*bm*-C*α*-PNA) forms a double duplex of the *bm*-PNA_2:DNA triplex. *J. Org. Chem.* **2021**, *86*, 414−428.
(63) Bhingardeve, P.; Jain, P.; Ganesh, K. N. Molecular assembly of triplex of duplexes from homothyminyl-homocytosinyl C*γ*(S/R)-bimodal peptide nucleic acids with dA_8/dG_6 and the cell permeability of bimodal peptide nucleic acids. *ACS Omega* **2021**, *6*, 19757−19770.
(64) Manicardi, A.; Rozzi, A.; Korom, S.; Corradini, R. Building on the peptide nucleic acid (PNA) scaffold: a biomolecular engineering approach. *Supramol. Chem.* **2017**, *29*, 784−795.
(65) Duan, T.; He, L.; Tokura, Y.; Liu, X.; Wu, Y.; Shi, Z. Construction of tunable peptide nucleic acid junctions. *Chem. Commun.* **2018**, *54*, 2846−2849.
(66) Swenson, C. S.; Velusamy, A.; Argueta-Gonzalez, H. S.; Heemstra, J. M. Bilingual Peptide Nucleic Acids: Encoding the languages of nucleic acids and proteins in a single self-assembling biopolymer. *J. Am. Chem. Soc.* **2019**, *141*, 19038−19047.
(67) Kumar, S.; Pearse, A.; Liu, Y.; Taylor, R. E. Modular self-assembly of gamma-modified peptide nucleic acids in organic solvent mixtures. *Nat. Commun.* **2020**, *11*, No. 2960.

https://doi.org/10.1021/acsomega.2c05873
ACS Omega 2022, 7, 40558−40568

(68) Zhan, X.; Deng, L.; Chen, G. Mechanisms and applications of peptide nucleic acids selectively binding to double-stranded RNA. *Biopolymers* **2022**, *113*, No. e23476.
(69) Yavin, E. Peptide Nucleic Acids: Applications in Biomedical Sciences. *Molecules* **2020**, *25*, 3317−3321.
(70) Das, A.; Pradhan, B. Evolution of peptide nucleic acid with modifications of its backbone and application in biotechnology. *Chem. Biol. Drug Design* **2021**, *97*, 865−892.
(71) Wojciechowska, M.; Równicki, M.; Mieczkowski, A.; Miszkiewicz, J.; Trylska, J. Antibacterial peptide nucleic acids: facts and perspectives. *Molecules* **2020**, *25*, 559−581.
(72) Talele, T. T. Natural products inspired use of the gem-dimethyl group in medicinal chemistry. *J. Med. Chem.* **2018**, *61*, 2166−2210.

https://doi.org/10.1021/acsomega.2c05873
ACS Omega 2022, 7, 40558−40568